Mössbauer study of Cr-based chalcogenide spinels $Fe_{1-x}Cu_xCr_2S_4$

Z. Klencsár[1*], E. Kuzmann[1], Z. Homonnay[2], Z. Németh[2], I. Virág[3], M. Kühberger[4], G. Gritzner[4], A. Vértes[1,2]

[1]*Research Group for Nuclear Methods in Structural Chemistry, Hungarian Academy of Sciences, Department of Nuclear Chemistry, Eötvös Loránd University, Pázmány P. s. 1/a, Budapest 1117, Hungary*
[2]*Department of Nuclear Chemistry, Eötvös Loránd University, Pázmány P. s. 1/a, Budapest 1117, Hungary*
[3]*Department of Inorganic and Analytical Chemistry, Eötvös Loránd University, Pázmány P. s. 1/a, Budapest 1117, Hungary*
[4]*Institut für Chemische Technologie Anorganischer Stoffe, Johannes Kepler Universität, A-4040 Linz, Austria*

Abstract

We report on the magnetic and electronic state of iron in Cu-substituted Cr-based thiospinels of the nominal composition $Fe_{1-x}Cu_xCr_2S_4$ ($x = 0.25,\ 0.5,\ 0.75$), a class of compounds which recently raised considerable interest in relation with the colossal magnetoresistance effect they display. ^{57}Fe Mössbauer measurements carried out at different temperatures revealed the gradual transformation of iron from the state of Fe^{2+} (representative for $x = 0$) to the state of Fe^{3+} (representative for $x \geq 0.5$), along with a simultaneous increase in the magnetic ordering temperature. In $Fe_{0.75}Cu_{0.25}Cr_2S_4$, where Fe^{2+} and Fe^{3+} oxidation states were found to coexist, the Mössbauer-Lamb factor characteristic of Fe^{3+} sites was found to exceed that characteristic of Fe^{2+} sites. Special attention is paid to the composition with $x = 0.5$. This compound was found to display a Curie temperature $T_C \approx 340$ K, a value which considerably exceeds the recently reported T_C value for a single crystal with the same average composition.

Introduction

Associated with the transition from the paramagnetic insulating phase to the ferromagnetic metal phase, observed in some materials, an effect known as 'colossal magnetoresistance (CMR)' occurs [1,2,3,4]. Near the transition temperature there is a significant change in resistance in response to an applied magnetic field in these materials. The first compounds found to show this effect were manganese oxides with the perovskite structure [5].

The large magnetoresistive effect observed recently in the Cr-based chalcogenide spinel class of materials [6] raised considerable interest in this field of research, particularly because

the discovery of the CMR effect in these compounds opens up a vast range of materials for the further exploration of the CMR phenomenon.

The mechanism of the CMR effect is thought to involve a strong correlation between the electronic, magnetic, and vibrational states of the ions present in the material. In the case of iron containing CMR materials ^{57}Fe Mössbauer spectroscopy enables us to study these properties, provided the state of the iron cations plays a role in the realization of the CMR effect. Mössbauer spectroscopy, that has already been used with success to study the electronic structure of chalcogenide spinels [7,8,9,10,11,12,13], may reveal the aforementioned correlations, as already found for $FeCr_2S_4$ [14,15] and Sr_2FeMoO_6 [16]. In this article we report on the characterization and ^{57}Fe Mössbauer study of the spinel compounds $Fe_{1-x}Cu_xCr_2S_4$, by focusing our attention on the compound with $x = 0.5$ that was shown to display CMR properties [6]. The Mössbauer technique was used for the study of chalcogenide spinels already several decades ago.

Experimental

The $Fe_{1-x}Cu_xCr_2S_4$ specimens were produced by solid state reactions. Fe and Cu (powder, p. A., Merck, Germany) were mixed together with Cr (300 μm, Merck, Germany) and S (DAB7, Merck, Germany) in exact stoichiometric ratios, and ground in an agate mortar. The resulted powders were compacted at a pressure of 500 MPa into pellets of 1 cm diameter. The pellets were then cut into half and placed inside a quartz tube with an outer diameter of 10 mm and a wall thickness of 2 mm. The tube was evacuated and sealed. The samples were then fired at 850°C for 12 h. The heating rate was 5 K min^{-1}. The resulted material was ground, and the obtained powder was again pressed into pellets with 10 mm diameter, which then were heat-treated a second time with the temperature program given above.

The samples were analyzed by X-ray diffraction (Geigerflex D-max II a, Rigaku, Japan) and by scanning electron microscopy (JSM-6400, JEOL) in combination with energy dispersive X-ray fluorescence spectroscopy (Röntec, Germany). The temperature dependence and the magnetic field dependence of the resistance were measured by the four point method.

^{57}Fe Mössbauer spectroscopy measurements were carried out on the $Fe_xCu_{1-x}Cr_2S_4$ ($x = 0.25, 0.5, 0.75$) samples in transmission geometry with a conventional constant acceleration type spectrometer. The γ-rays were provided by a ^{57}Co(Rh) Mössbauer source with an activity of ~ 10^9 Bq. The temperature dependence of the spectra was measured in a flow-through type liquid nitrogen cryostat (Leybold). The precision of temperature regulation

* Corresponding author.

was ±0.5 K. ^{57}Fe isomer shifts are given relative to α-iron at room temperature. Mössbauer spectra were analyzed with version 3.0i of the MossWinn program [17].

Results and discussions

Figure 1 shows the X-ray diffraction patterns of a series of samples with the nominal composition of $Fe_{1-x}Cu_xCr_2S_4$ ($x = 0$, 0.25, 0.5, 0.75). The copper free sample is quite phase pure. Only a small amount of Cr_2S_3 could be identified in the X-ray diffractogram. The formation of Cr_2S_3 is believed to have its origin in the quite big diameter (~ 300 μm) of the Cr particles. Since it is not possible to grind ductile metals perfectly in a mortar, this step may be seen as a homogenization step rather than a grinding step. The reaction is believed to take place within the quartz tube, first in liquid sulfur, then by a reaction with sulfur vapor. Sulfur reacts also with pure Cr while the thiospinel phase is forming.

By adding copper to the system, a third phase, identified as $CuCrS_2$ [18], was formed. The best crystallized sample with the highest phase purity could be obtained for the composition $Fe_{0.5}Cu_{0.5}Cr_2S_4$. By substituting parts of Fe in the spinel lattice by Cu, a shift of the XRD reflections to higher 2θ values could be observed for $x = 0.25$ and $x = 0.5$, reflecting a decrease in the lattice spacings in agreement with results published in [19]. The diffractogram of the sample with $x = 0.75$ shows a high amount of $CuCrS_2$ impurity phase, referring to a decrease in the Cu content of the corresponding spinel phase.

The scanning electron micrographs of $Fe_{0.5}Cu_{0.5}Cr_2S_4$ shown in Figure 2 display triangle shaped crystallites typical for compounds with the spinel structure. The characteristic size of the crystallites is below 20 μm. Comparison of the surface (Figure 2a) and the section of an inner part (Figure 2b) of the sample refers to a homogenous crystallization all over the specimen. The result of energy dispersive fluorescence analysis carried out on a crystallite (point X in Figure 2a) is given in Figure 3. A corresponding computer calculation of the concentrations for the individual elements (using the software "Win-Shell") yielded the formula $Fe_{0.5}Cu_{0.5}Cr_2S_4$ within experimental error.

Figure 4 shows the temperature dependence of the electrical resistance of $Fe_{0.5}Cu_{0.5}Cr_2S_4$. Below about $T \approx 100$ K electrical resistance starts to increase steeply with decreasing temperature, a sign for an insulating ground state of the material. The minimum in the electrical resistance around $T \approx 140$ K is in agreement with corresponding single crystal data [19] indicating that the temperature dependence of the electrical resistance of our polycrystalline material reflects the corresponding property of the crystallites (Figure 2). The magnetic field dependence of the electrical resistance of $Fe_{0.5}Cu_{0.5}Cr_2S_4$, shown in Figure 5,

was measured at $T = 77$ K. A relatively low negative magnetoresistance is observed, whose magnitude increases steeply with increasing magnetic field for $B < 0.5$ T, and seems to get saturated at higher magnetic field values. This is also in agreement with corresponding single crystal data recorded at the same temperature [19]. The agreement of our data obtained for polycrystalline $Fe_{0.5}Cu_{0.5}Cr_2S_4$ with those obtained for single crystal specimen indicates that the inter-grain junctions in the polycrystalline material are well crystallized, and display transport properties similar to those of the individual crystallites.

Figure 6 shows the ^{57}Fe Mössbauer spectra of the samples $Fe_{1-x}Cu_xCr_2S_4$ for $x = 0.25$, 0.5 and 0.75, measured at $T \approx 77$ K as well as at room temperature. At room temperature, a paramagnetic spectrum is observed for $x = 0.25$. A magnetic six line pattern besides a minor paramagnetic doublet component (see Table 1) is the characteristic feature of the spectra for $x = 0.5$ and $x = 0.75$, indicating that the Curie temperature is above room temperature for the latter two compounds. Furthermore, the room temperature hyperfine magnetic field reflected by the sextet characteristic for the sample with $x = 0.75$ ($B = 25.26(4)$ T) exceeds that characteristic for the sample with $x = 0.5$ ($B = 24.47(2)$ T). This suggests that the Curie temperature is further increased with an increase in x from 0.5 to 0.75. The isomer shift of the sextet is around ~ 0.3 mm/s for both compounds (see Table 1), clearly indicating that iron exists exclusively in the Fe^{3+} oxidation state in the compounds with $x \geq 0.5$.

Beside the magnetic sextet, the Mössbauer spectra of the studied samples contain minor paramagnetic components as well. Because of the overlap with the inner two peaks of the magnetic sextet component, the Mössbauer parameters of these paramagnetic components cannot be determined unambiguously. For this reason, in Table 1 and Table 2 we give only their relative spectral area as well as their isomer shift along with the corresponding oxidation state of iron. These minor paramagnetic components may originate from iron being situated in the neighborhood of a sulfur vacancy in the spinel structure itself, or they may be a sign of a minority sulfide phase outside the spinel. FeS_2 both as pyrite and as marcasite [20, 21] and even superparamagnetic FeS can result in similar paramagnetic Mössbauer spectra [21, 22, 23,24].

As shown by Table 1, the compound with $x = 0.25$, being paramagnetic at room temperature, displays a Mössbauer spectrum that actually consists of two paramagnetic components. One component has an isomer shift of $\delta \approx 0.40$ mm/s, a value which refers to iron in the Fe^{3+} oxidation state, the other has an isomer shift $\delta \approx 0.66$ mm/s, a value representative for iron in the Fe^{2+} oxidation state in the tetrahedral site of $FeCr_2S_4$ [14]. Thus, substitution of iron by copper in $Fe_{1-x}Cu_xCr_2S_4$ at low copper concentrations results in a

gradual transformation of Fe^{2+} to Fe^{3+}. This transformation seems to happen in a rather homogeneous manner, without the formation of crystallites with considerably higher or lower concentration of copper compared to the average stoichiometry. If crystallites with an average composition of $Fe_{0.5}Cu_{0.5}Cr_2S_4$ existed in the sample with $x = 0.25$ then, according to Figure 6 and Table 1, at room temperature a magnetic sextet belonging to these crystallites should show up in the Mössbauer spectrum. This is not the case (Figure 6). The existence of two different oxidation states of iron in $Fe_{0.75}Cu_{0.25}Cr_2S_4$ is also clearly apparent in the Mössbauer spectrum recorded at $T \approx 77$ K (Figure 6). The sextet belonging to Fe^{3+} sites and that belonging to Fe^{2+} sites can be clearly distinguished on the basis of the considerably different hyperfine magnetic fields (~ 33 T vs. ~ 22.6 T, respectively) which they reflect (Table 2). The formation of Fe^{3+} as a result of Cu substitution also indicates that copper exists in the Cu^{+} oxidation state in this system.

Figure 7 shows Mössbauer spectra of $Fe_{0.5}Cu_{0.5}Cr_2S_4$ at selected temperatures of interest. In order to achieve a more precise fit of the main magnetic component, the minor paramagnetic components in these spectra were fitted by a model-independent way as a distribution of singlet peaks. Therefore the paramagnetic components in Figure 7 are displayed only by the envelope of their sum, without further resolving the singlet and/or doublet subcomponents that may have contributed to them. On the basis of the spectra recorded in the temperature range $325 \text{ K} < T < 340 \text{ K}$ it is clear that in $Fe_{0.5}Cu_{0.5}Cr_2S_4$ the magnetic order breaks down anomalously. A paramagnetic component exists together with the magnetic one below the Curie temperature in an intermediate temperature region. This anomalous behavior seems to be characteristic of iron containing CMR materials [14,15]. It was observed in $FeCr_2S_4$ in an even more pronounced manner [14]. Such a magnetic transition reflects, that by approaching T_C from below, the bulk magnetic material gradually breaks down into smaller and smaller individual magnetic domains which, after reaching a critical size (in the order of ~ 10 nm), behave like superparamagnetic particles [25]. Since the relaxation rate of the magnetic moment of these domains exceeds the Larmor precession rate of the ^{57}Fe nucleus (~ 10^7 1/s), they will give rise to a paramagnetic singlet or doublet component in the ^{57}Fe Mössbauer spectrum, even at temperatures below T_C. A distribution in the size of these domains furthermore leads to a distribution in the hyperfine magnetic field already before the collapsed paramagnetic peak appears. This effect is also clearly visible in the Mössbauer spectra of $Fe_{0.5}Cu_{0.5}Cr_2S_4$ taken at temperatures in the range from 320 K to 330 K (Figure 7). The formation of these nanosized magnetic clusters, as well as their alignment as a response to an externally applied magnetic field, is thought to play a role in the

realization of a pronounced CMR effect in the neighborhood of the Curie temperature in CMR materials [15, 26].

As reflected also by Figure 8, the Curie temperature of polycrystalline $Fe_{0.5}Cu_{0.5}Cr_2S_4$ material is $T_C \approx 340$ K, which is in sharp contrast with the value $T_C \approx 275$ K reported in [19] for single crystal $Fe_{0.5}Cu_{0.5}Cr_2S_4$, but in agreement with data published earlier for polycrystalline $Fe_{0.5}Cu_{0.5}Cr_2S_4$ [6]. (Emission Mössbauer spectroscopy measurements performed on ^{57}Co doped $Fe_{0.5}Cu_{0.5}Cr_2S_4$ single crystal may be helpful in resolving the controversy concerning the different Curie temperatures of single crystal and polycrystalline $Fe_{0.5}Cu_{0.5}Cr_2S_4$.)

The ^{57}Fe isomer shifts of $Fe_{0.25}Cu_{0.75}Cr_2S_4$ and $Fe_{0.5}Cu_{0.5}Cr_2S_4$ are practically the same, which means that the effect of the Cu substitution on the electronic structure of iron is saturated at $x = 0.5$. The excess part of copper over $x = 0.5$ should have the Cu^{2+} state. Nevertheless, it can not be excluded that a part of the excess copper remains in the form of mono-valent Cu and sulfur vacancies are formed in the crystal lattice.

The Mössbauer spectrum of the sample with $x = 0.25$ (Figure 6) displays an $Fe^{2+} : Fe^{3+}$ ratio that changes with temperature (see Table 1 and Table 2). Based on the requirement of charge neutrality, assuming that all the copper in the sample is in the Cu^{+} state, one would expect the relative amount of Fe^{2+} and Fe^{3+} to be $Fe^{2+} : Fe^{3+} = 2 : 1$. The room temperature ^{57}Fe Mössbauer spectrum of $Fe_{0.75}Cu_{0.25}Cr_2S_4$ (Figure 6) is, however, not in agreement with this expectation. A comparison of the peak areas belonging to Fe^{2+} and Fe^{3+} yields a ratio of $Fe^{2+} : Fe^{3+} \approx 1 : 2.2$. One should consider, however, that the ratio of Mössbauer peak areas reflects the relative occurrence of the corresponding iron species only if the recoilless fraction (the probability of the Mössbauer effect, also called the Mössbauer-Lamb factor) is the same for the two species. Since the recoilless fraction should have a tendency to approach 100% with decreasing temperature for all species, a Mössbauer measurement carried out at a lower temperature should result in a Mössbauer spectrum in which the area ratio of the peaks reflects the relative occurrence of the corresponding iron species better than it does in the case of the measurement at room temperature. The Mössbauer spectrum at $T = 77$ K (Figure 6) can be decomposed into three different components. The component belonging to Fe^{2+} is a magnetically split sextet ($\delta = 0.65(2)$, $B = 22.6(2)$ T). In addition, we observe two different subspectra with parameters representative for Fe^{3+}. One of them is a magnetically split sextet ($\delta = 0.51(1)$, $B = 33.0(1)$ T), whereas the other is a paramagnetic component (having a relative area fraction of ~ 9%) with $\delta = 0.55(2)$ referring to Fe^{3+} cations in the paramagnetic state. The nearly equal isomer shift

of the two different Fe^{3+} components suggests that the corresponding cations may be situated in the same crystallographic position in $Fe_{0.75}Cu_{0.25}Cr_2S_4$, but the iron cations belonging to the paramagnetic component are probably separated from the magnetically ordered regions (e.g. by sulfur vacancies) and consequently they display paramagnetic behavior at $T = 77$ K.

By analyzing the area ratio of the subspectra belonging to Fe^{2+} and Fe^{3+} cations in the Mössbauer spectrum taken at $T = 77$ K, one observes a ratio $Fe^{2+} : Fe^{3+} \approx 3 : 2$. This ratio is closer to the expected ratio 2 : 1 than that observed at room temperature (1 : 2.2). The significant difference between the apparent $Fe^{2+} : Fe^{3+}$ ratios observed at room temperature and at $T = 77$ K indicates that in $Fe_{0.75}Cu_{0.25}Cr_2S_4$ at room temperature the Mössbauer-Lamb factor belonging to Fe^{3+} is at least three times of that belonging to Fe^{2+}. This result shows that by replacing iron with copper in $Fe_{1-x}Cu_xCr_2S_4$ it is not only the oxidation state of iron that changes, but simultaneously with the transition $Fe^{2+} \rightarrow Fe^{3+}$ the local vibrational state of iron cations is altered considerably, too.

Conclusions

^{57}Fe Mössbauer spectroscopy of Cu substituted $Fe_{1-x}Cu_xCr_2S_4$ spinel samples revealed that the substitution of iron with copper happens in a homogeneous manner in these compounds. In agreement with a Cu^+ copper oxidation state, Cu substitution was found to result in a gradual transformation of Fe^{2+} to Fe^{3+}. At low ($x = 0.25$) Cu concentration, Fe^{2+} and Fe^{3+} were found to coexist in the system. The temperature dependence of the relative spectral areas of Fe^{2+} and Fe^{3+} components in the Mössbauer spectra of $Fe_{0.75}Cu_{0.25}Cr_2S_4$ revealed that in comparison with Fe^{2+} sites, at a given temperature Fe^{3+} sites are characterized by a larger Mössbauer-Lamb factor, which in these compounds may lead to an excessive overestimation of the relative amount of Fe^{3+} sites, especially if the latter is determined exclusively on the basis of a room temperature Mössbauer measurement.

Detailed studies of the ^{57}Fe Mössbauer spectra of $Fe_{0.5}Cu_{0.5}Cr_2S_4$ revealed a Curie temperature of $T_C \approx 340$ K, which considerably exceeds the published values for single crystals [19]. Just below the Curie temperature, the magnetic order of $Fe_{0.5}Cu_{0.5}Cr_2S_4$ was found to break down anomalously forming small (~ 10 nm) superparamagnetic clusters, which gradually shrink in size as the temperature approaches T_C from below. In the Mössbauer spectra this process results in a premature collapse of the magnetic six line pattern and leads to the appearance of a paramagnetic peak well below T_C.

Acknowledgement

This work was supported by the Hungarian Science Foundation OTKA (F 034837, T 043565, and T 034839) as well as by the Wissenschaftlich-Technische Zusammenarbeit Österreich Ungarn project A-22/01. The authors are thankful to Mr. Ferenc Árva for his experimental contribution in recording Mössbauer spectra. Z. Klencsár acknowledges the support from the Hungarian Bolyai János research grant.

References

[1] S. Jin, T. H. Tiefel, M. McCormick, R. A. Fastnacht, R. Ramesh, L. H. Chen, *Science* **264** (1994) 413.

[2] R. von Helmholt, J. Wecker, B. Holzafel, L. Schultz, K. Samwer, *Phys. Rev. Lett.* **71** (1993) 2331.

[3] K. Chahara, T. Ohno, M. Kasai, Y. Kozono, *Appl. Phys. Lett.* **63** (1993) 1990.

[4] R. M. Kusters, J. Singleton, D. A. Keen, R. L. McGreevy, W. Hayes, *Physica B* **155** (1989) 362.

[5] G. H. Jonker, J. H. Van Santen, *Physica* **16** (1950) 337.

[6] A. P. Ramirez, R.J. Cava, J. Krajewski, *Nature* **386** (1997) 156.

[7] M. Eibschutz, S. Shtrikman, Y. Tenenbaum, *Phys. Lett.* **24A** (1967) 563.

[8] G. R. Hoy, S. Chandra, *J. Chem. Phys.* **47** (1967) 961.

[9] G. R. Hoy, K. P. Singh, *Phys. Rev.* **172** (1968) 514.

[10] G. Haacke, A. J. Nozik, *Solid State Commun.* **6** (1968) 363.

[11] C. M. Yagnik, H.B. Mathur, *Solid State Commun*. **5** (1967) 841.

[12] L. Brossard, J. L. Dormann, L. Goldstein, P. Gibart, P. Renaudin, *Phys. Rev. B* **20** (1979) 2933.

[13] O. Lang, C. Felser, R. Seshadri, F. Renz, J.M. Kiat, J. Ensling, P. Gütlich, W. Tremel, *Advanced Materials* **12** (2000) 65.

[14] Z. Klencsár, E. Kuzmann, Z. Homonnay, A. Vértes, A. Simopoulos, E. Devlin, G. Kallias, *J. Phys. Chem. Solids* **64** (2003) 325.

[15] A. Nath, Z. Klencsár, E. Kuzmann, Z. Homonnay, A. Vértes, A. Simopoulos, E. Devlin, G. Kallias, A. P. Ramirez, R. J. Cava, *Physical Review* B **66** (2002) 212401.

[16] Z. Klencsár, Z. Németh, A. Vértes, I. Kotsis, M. Nagy, Á. Cziráki, C. Ulhaq-Bouillet, V. Pierron-Bohnes, K. Vad, S. Mészáros, J. Hakl, *J. Magn. Mag. Mat.* **281** (2004) 115.

[17] Z. Klencsár, E. Kuzmann, A. Vértes, *J. Rad. Nucl. Chem.* **210**, No. 1. (1996) 105.

[18] (ICCD code 83-1690).

[19] V. Fritsch, J. Deisenhofer, R. Fichtl, J. Hemberger, H.-A. Krug von Nidda, M. Mücksch, M. Nicklas, D. Samusi, J. D. Thompson, R. Tidecks, V. Tsurkan, A. Loidl, *Phys. Rev.* B **67** (2003) 144419.

[20] A. Temperly, H. W. Lefevre, *J. Phys. and Chem. Solids* **27** (1966) 85.

[21] J. A. Morice, L. V. C. Rees, D. T. Rickard, *J. Inorg. Nuclear Chem.* **31** (1969) 3797.

[22] K. Ono, A. Ito, E. Hirahara, *J. Phys. Soc. Japan*, 17, 1615 (1962)

[23] K. Ono, Y. Ishikawa, A. Ito, E. Hirahara, *J. Phys. Soc. Japan*, 17, Suppl. B-I, 125 (1962)

[24] S. S. Hafner, B. J. Evans, G. M. Kalvius, *Solid State Commun.*, 5, 17 (1967)

[25] L. M. Levinson, M. Luban, S. Shtrikman: *Phys. Rev.* **177** (1969) 864.

[26] Z. Klencsár, E. Kuzmann, Z. Homonnay, A. Vértes, A. Simopoulos, E. Devlin, G. Kallias: *Hyperfine Interactions* **144/145** (2002) 261.

Table 1. Room temperature Mössbauer parameters of $Fe_{1-x}Cu_xCr_2S_4$. Relative subspectrum areas (as percentage values) are indicated in parentheses. Data concerning $FeCr_2S_4$ ($x = 0$) are based on measurements published in [14]. The letters δ, Δ and B denote the ^{57}Fe isomer shift (relative to α-iron), quadrupole splitting and hyperfine magnetic field Mössbauer parameters, respectively. In cases where an unambiguous identification of the paramagnetic component was not possible, only an estimation of the isomer shift of the paramagnetic component is given together with the corresponding iron oxidation state.

Sample	Magnetic component(s)	Paramagnetic component(s)
$Fe_{0.25}Cu_{0.75}Cr_2S_4$ ($x = 0.75$)	Fe^{3+} Sextet (83%) $\delta = 0.30(1)$ mm/s $B = 25.26(4)$ T	Fe^{3+} (17%) $\delta = 0.31(2)$ mm/s
$Fe_{0.5}Cu_{0.5}Cr_2S_4$ ($x = 0.5$)	Fe^{3+} Sextet (89%) $\delta = 0.308(3)$ mm/s $B = 24.47(2)$ T	Fe^{3+} (11%) $\delta = 0.35(5)$ mm/s
$Fe_{0.75}Cu_{0.25}Cr_2S_4$ ($x = 0.25$)		Fe^{2+} (31%) $\delta = 0.66(1)$ mm/s Fe^{3+} (69%) $\delta = 0.40(1)$ mm/s
$FeCr_2S_4$ ($x = 0$)		Fe^{2+} (100%) $\delta = 0.595(1)$ mm/s

Table 2. Mössbauer parameters of $Fe_{1-x}Cu_xCr_2S_4$ at $T \approx 77$ K. Relative subspectrum areas (as percentage values) are indicated in parentheses. Data concerning $FeCr_2S_4$ ($x = 0$) are based on measurements published in [14]. The letters δ, Δ and B denote the ^{57}Fe isomer shift (relative to α-iron), quadrupole splitting and hyperfine magnetic field Mössbauer parameters, respectively. In cases where an unambigous identification of the paramagnetic component was not possible, only an estimation of the isomer shift of the paramagnetic component is given together with the corresponding iron oxidation state.

Sample	Magnetic component(s)	Paramagnetic component(s)
$Fe_{0.25}Cu_{0.75}Cr_2S_4$ ($x = 0.75$)	Fe^{3+} Sextet (86%) $\delta = 0.42(1)$ mm/s $B = 37.3(4)$ T	Fe^{3+} (14%) $\delta = 0.31(2)$ mm/s
$Fe_{0.5}Cu_{0.5}Cr_2S_4$ ($x = 0.5$)	Fe^{3+} Sextet (90.5%) $\delta = 0.434(3)$ mm/s $B = 37.19(2)$ T	Fe^{3+} (9.5%) $\delta = 0.4(1)$ mm/s
$Fe_{0.75}Cu_{0.25}Cr_2S_4$ ($x = 0.25$)	Fe^{3+} Sextet (32%) $\delta = 0.51(1)$ mm/s $B = 33.0(1)$ T Fe^{2+} Sextet (59%) $\delta = 0.65(2)$ mm/s $B = 22.6(2)$ T	Fe^{3+} (9%) $\delta = 0.55(2)$ mm/s
$FeCr_2S_4$ ($x = 0$)	Sextet of regular tetrahedral Fe^{2+} (90%) $\delta = 0.71(1)$ mm/s $B = 20.00(4)$ T Sextet of tetrahedral Fe^{2+} in the neighborhood of a sulfur vacancy (6.3%) $\delta = 0.9(1)$ mm/s $B = 30.1(5)$ T $\Delta = -0.9(2)$ mm/s	Fe^{2+} Doublet (3.7%) $\delta = 0.7(1)$ mm/s $\Delta = 1.0(1)$ mm/s

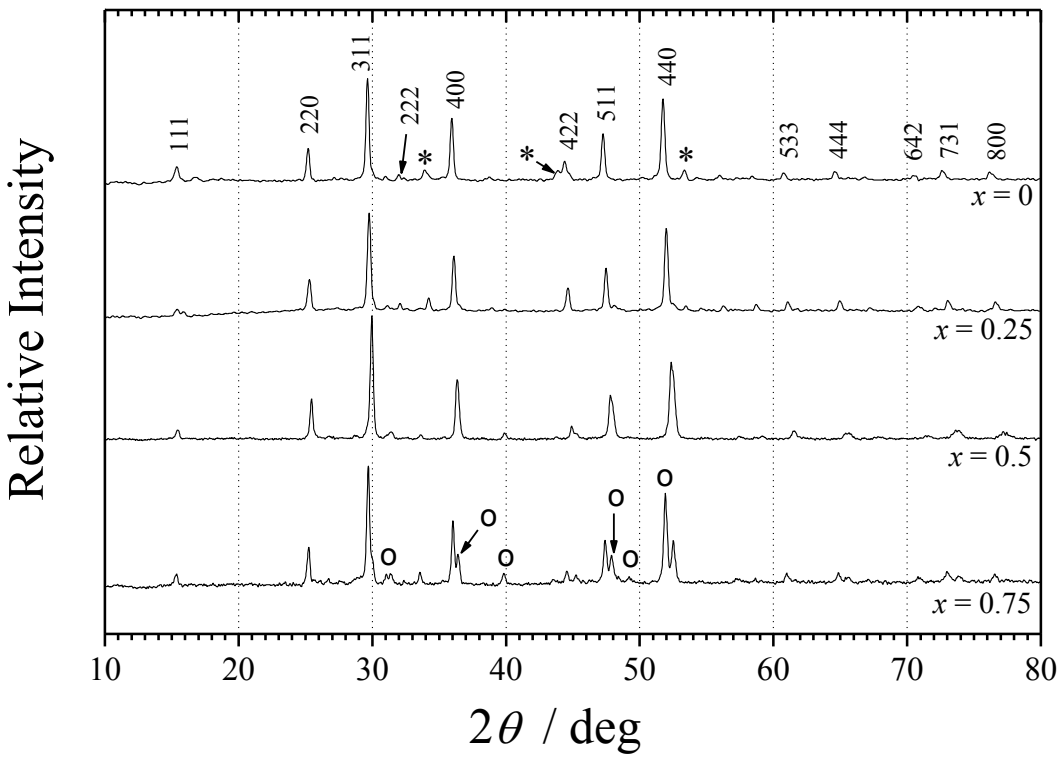

Figure 1. X-ray diffraction patterns of $Fe_{1-x}Cu_xCr_2S_4$ for $x = 0$, 0.25, 0.5 and 0.75, recorded by using Ni-filtered Cu K_α radiation. For $x = 0$ * signs indicate diffraction peaks belonging to Cr_2S_3 minority phase, and for $x = 0.75$ o signs mark peaks of the minority phase $CuCrS_2$. The hkl indexes are indicated only for $x = 0$.

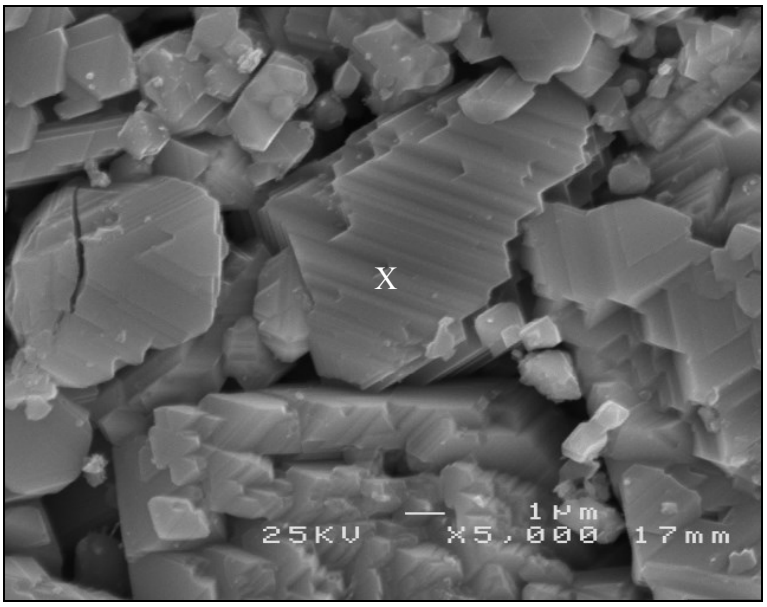

a

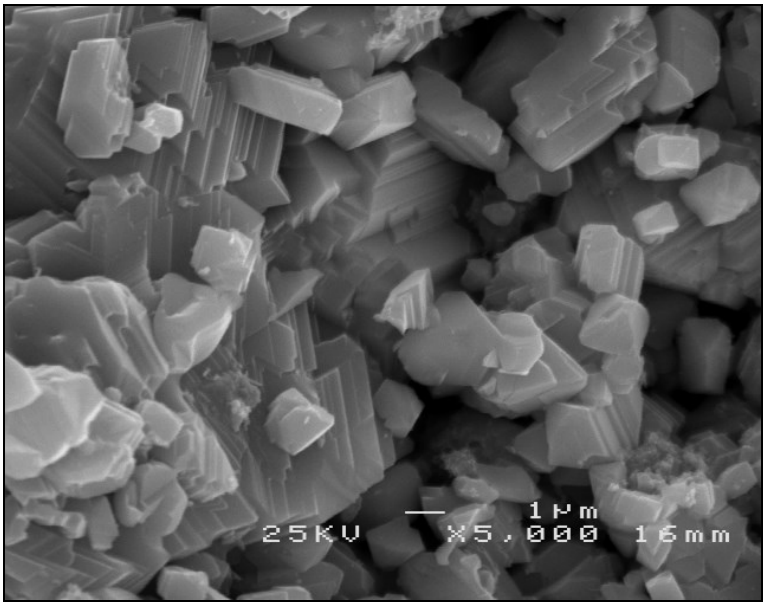

b

Figure 2. Scanning electron images of the surface (a) and an inner part of $Fe_{0.5}Cu_{0.5}Cr_2S_4$ (b). On part (a), X denotes the point where energy dispersive fluorescence analysis was performed (see Figure 3).

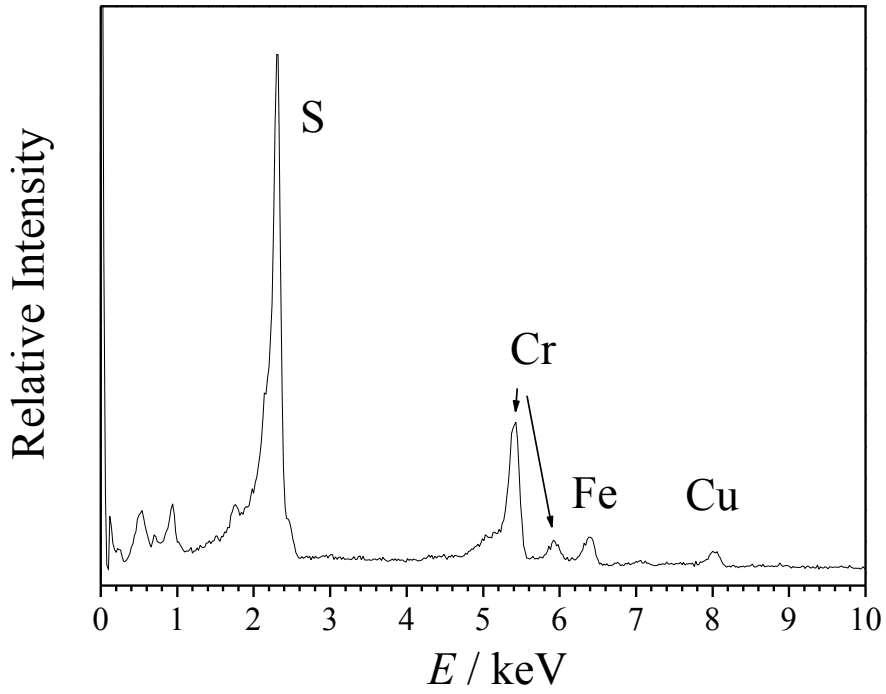

Figure 3. The result of the energy dispersive fluorescence analysis of a crystallite of $Fe_{0.5}Cu_{0.5}Cr_2S_4$ (point X in Figure 2a).

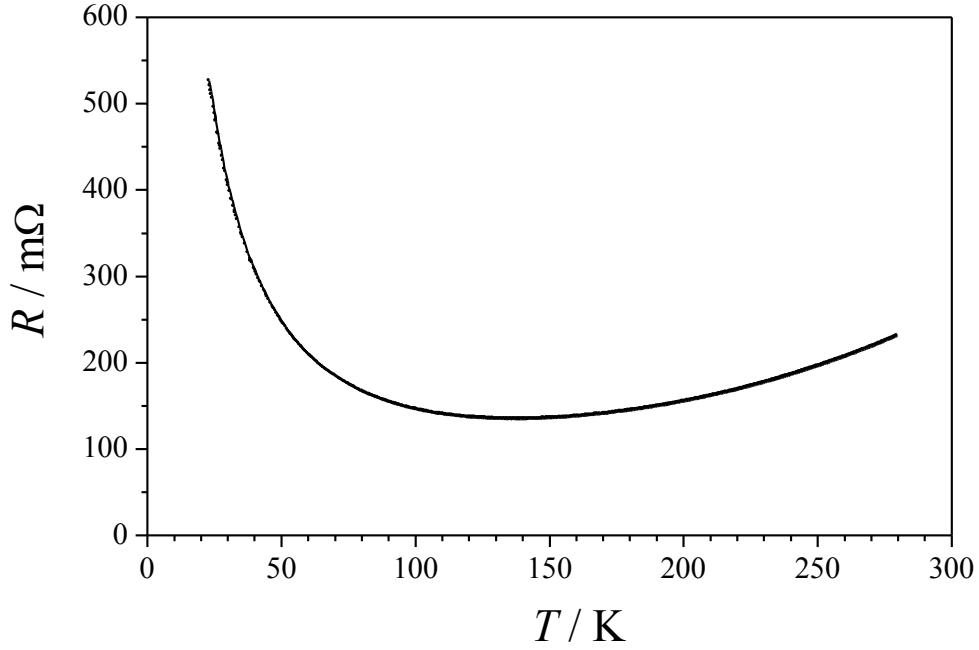

Figure 4. Temperature dependence of the electrical resistance of bulk polycrystalline $Fe_{0.5}Cu_{0.5}Cr_2S_4$.

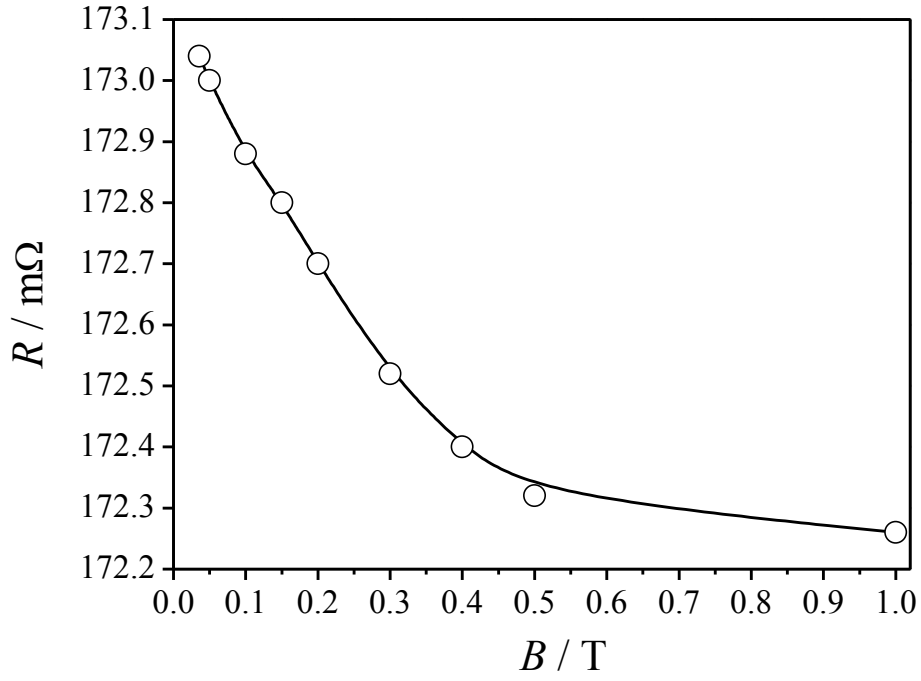

Figure 5. Magnetic field dependence of the resistance of $Fe_{0.5}Cu_{0.5}Cr_2S_4$ at 77 K. The line through the points is a guide to the eye.

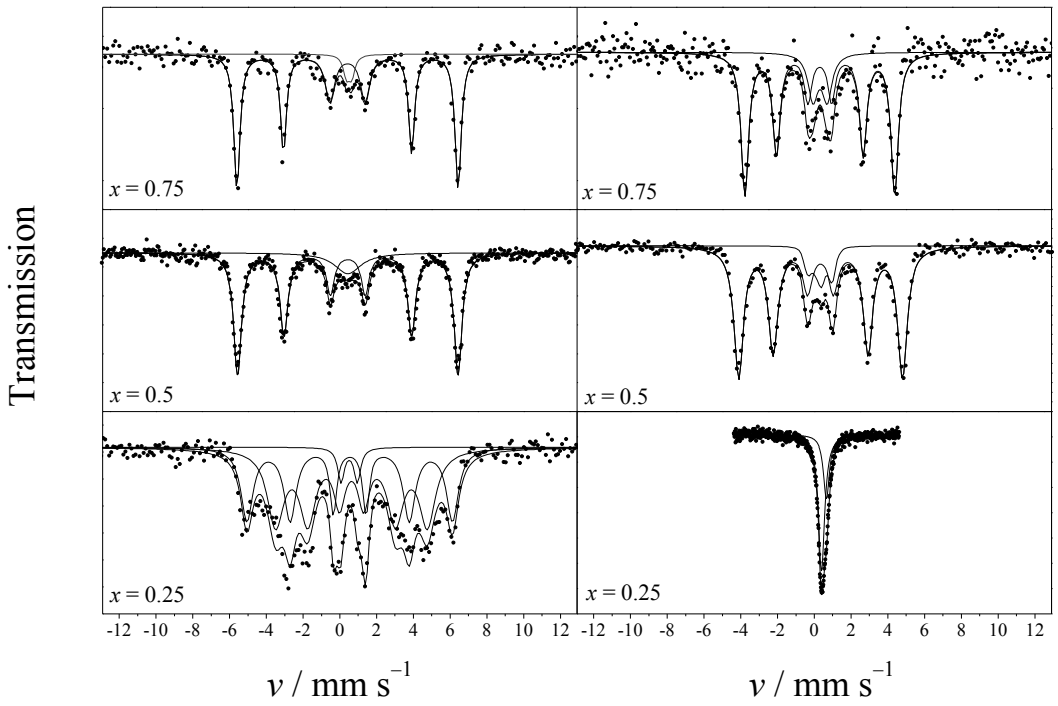

Figure 6. ^{57}Fe Mössbauer spectra of $Fe_{1-x}Cu_xCr_2S_4$ ($x = 0.25$, 0.5, 0.75) at $T \approx 77$ K (left column) and at room temperature (right column). In spectra reflecting magnetic splitting, only the envelope of the minority paramagnetic components is shown. The spectra on top of each other share a common velocity axis.

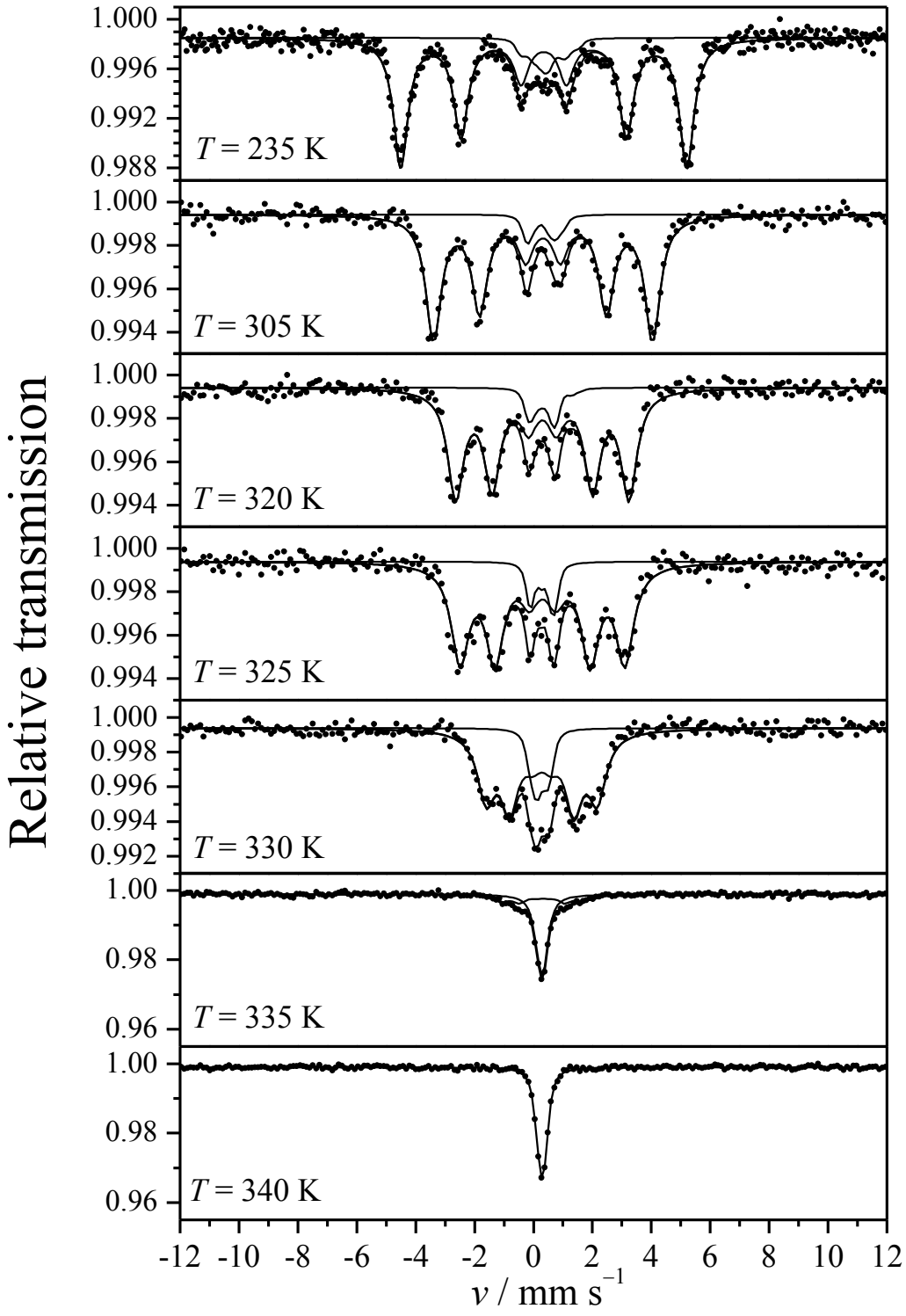

Figure 7. ^{57}Fe Mössbauer spectra of $Fe_{0.5}Cu_{0.5}Cr_2S_4$ at selected temperatures. For $T \leq 335$ K the spectra consist of a magnetic component together with one or more paramagnetic components. Paramagnetic components were fitted in a model-independent way, and it is only the envelope of their sum what is displayed in the figure. The spectra share a common velocity axis.

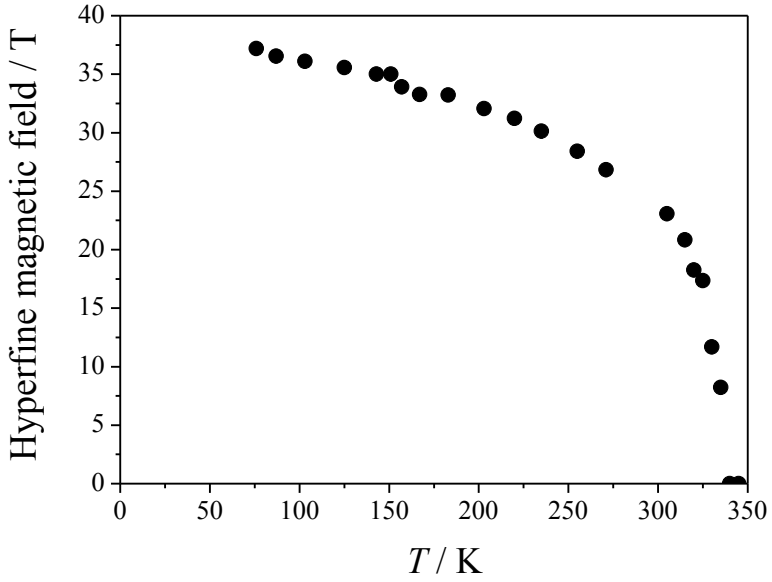

Figure 8. Temperature dependence of the hyperfine magnetic field displayed by the sextet component in the ^{57}Fe Mössbauer spectrum of $Fe_{0.5}Cu_{0.5}Cr_2S_4$. Standard deviation of the displayed values is lower than the size of the points.